EFFECT OF ALKALI LEACHING ON EXPANSION TESTS IN LABORATORY

Stéphane Multon[1]*, Alain Sellier[1]

[1]Université de Toulouse; UPS, INSA; LMDC (Laboratoire Matériaux et Durabilité des Constructions); 135, avenue de Rangueil; F-31 077 Toulouse Cedex 04, FRANCE

Abstract

Different methods have been proposed to reassess structures damaged by Alkali-Silica Reaction (ASR). Using potential expansions test on specimens drilled from affected structures is the most usual procedure. However representing expansion of massive structures by such laboratory tests is still in question and need more investigations. Indeed, expansions on structures appear often longer and larger. Several scale effects acting on ASR expansion lead to obtain larger expansions on larger specimens according to the storage conditions of the specimens: moisture, alkali leaching and gel permeation through cracks can explain such effects.

This paper presents a simplified modelling to take into account the alkali mass balance in and out of the specimens. Both the consumption of alkali by ASR-gel production and the decrease of alkali concentration in pore solution due to external leaching are considered and compared to literature data. The consequences on expansion will be evaluated through the coupling with mechanics effects. The quantification of the different scale effects on ASR expansion is important to analyze the results of expansion test performed in laboratory and the presented modeling could be useful to future diagnosis of ASR-damaged structures.

Keywords: alkali, leaching, expansion, modelling, scale effect

1 INTRODUCTION

Different methods have been proposed to reassess structures damaged by Alkali-Silica Reaction. Using expansions tests on specimens drilled from structures is the most usual procedure. However, the use of results provided by these procedures is still under debate due to scale effects. Alkali leaching [1]–[3], moisture gradient [4] and ASR-gel permeation [5], [6] lead to larger expansions in larger specimens according to the storage conditions. These phenomena impact the ASR-expansion measured on specimens, and raises the question of whether such measurements should be used to represent expansion attained by affected aging structures. In order to obtain a better prediction of expansion in structures, models have to be able to distinguish the portion of the scale effect which exists due to alkali leaching as well as the portion that is induced by gel permeation through cracks. Expansion tests in conditions close to structural environment are performed under constant moisture. For such experiments, one of the main scale effects may be the alkalis leaching. This paper focuses on the alkali mass balance in ASR mechanisms and proposes a modelling to reproduce the effect of alkali leaching on the expansion of prisms. A multi-scale chemical approach is proposed to quantify alkali actions:

- At the aggregate scale, the mass balance equation of alkalis considers the diffusion and fixation in ASR-gels in the aggregate particles,
- At the concrete scale, the mass balance considers the alkali diffusion in a specimen, while the alkali consumption in the specimen is evaluated from the previous scale.

The link between chemical modelling and expansion is obtained through a model based on poromechanical theory that takes into account creep and damage at the concrete scale. Finally, a case study is presented to analyze literature experiments involving scale effects due to alkali leaching and consequences on measured expansion are discussed.

2 MULTI-SCALE APPROACH

The alkali mass balance is performed at two scales: the aggregate and the concrete scales (Figure 1). At the aggregate scale, the alkali mass balance equation considers the diffusion and the fixation of alkali in ASR-gels. To be representative of the different types of aggregate attacks [7], [8], analysis of ASR cannot consider the alkali diffusion in reactive aggregate as the only driving

*Correspondence to: stephane.multon@insa-toulouse.fr

mechanism of ASR-kinetics. At least two main phenomena should be taken into consideration (Figure 1): ionic transport (having alkali and silica in the same place) and the chemical reaction (attack of silica to form ASR-gel). At concrete scale, the alkali diffusion equation takes the alkali flow $\overrightarrow{\varphi_{Na}^{c}}$ due to external boundary conditions into account (Figure 1). The alkali bound in ASR-gels ($S_{\sum Na_b}^{c}$ in Figure 1) can be evaluated as the sum of alkali flow at the boundary of the aggregate determined at the lower scale. The alkali concentration in the cement paste at the aggregate edge and at the concrete scale ([Na+]x in Figure 1) has to be the same to obtain consistent multi-scale approach.

2.1 Aggregate scale

Alkali transport

The reactive silica is attacked in presence of hydroxyl and alkali ions before ASR-gels are formed. In most cases, alkali and hydroxyl come from the cement paste solution and move to the silica in the aggregate to start the reaction. The mass balance equation at aggregate scale represents the diffusion in aggregates and the fixation in ASR-gels. It is applied for each size of aggregate, as proposed in previous modelling [9], [10]. It can be written, for a constant water saturation degree:

$$p_{agg} S_r \frac{\partial [Na^+]}{\partial t} = -\mathrm{div}\left(\overrightarrow{\varphi_{Na}^{agg}}\right) + S_{Na} \quad (1)$$

with p_{agg} the aggregate porosity, S_r the degree of water saturation, $[Na^+]$ the alkali concentration in solution, $\overrightarrow{\varphi_{Na}^{agg}}$ the alkali flow in the aggregate and S_{Na}, the rate of alkali binding in ASR-gels per unit of time and of aggregate volume. The alkali flow depends on the coefficient of diffusion of alkali in the aggregate D_{agg}:

Alkali transport might depend on the location of the reactive silica (in contact with cracks or contained in veins of the aggregates [7]). For the sake of simplicity, the coefficient of diffusion is assumed to be homogeneous in the aggregate. It leads to discrepancy with reality and a calibration by inverse analysis of the expansion curves is required. The dependence of the expansion kinetics on the aggregate sizes can be reproduced by the use of this equation which leads to differences of alkali ingress into the aggregate.

Fixation in gels

The rate of alkali fixation in ASR-gels (S_{Na} in the mass balance equation applied at the aggregate scale) is driven by the reactivity of the aggregate. It is assumed that linear kinetics is sufficient to consider the silica attack and the ASR-gel precipitation according to an alkali threshold [11]. This is a simplified approach compatible with experimental results on pore solution extraction [12].

$$S_{Na} = -\frac{\partial Na_f}{\partial t} = -\frac{\langle [Na^+] - [Na^+]_{(Ca,T)}^{thr} \rangle^+}{\tau_{ASR}} \quad (2)$$

with τ_{ASR} the characteristic time of silica attack, which represents silica reactivity (in reality, it depends on the combination of both the kinetics of the reactive silica dissolution and the kinetics of the ASR-gel production) and $[Na^+]_{(Ca,T)}^{thr}$ the alkali concentration "threshold" below which the reaction products cause negligible expansion. In the first version of this model [11], considering a constant threshold of alkali in equation (3) was sufficient to model ASR-expansion of concrete with different alkali contents in moisture conditions [11]. However, it leads to expansion rates quite different for the expansion of specimens kept in NaOH solution. No threshold was selected for such calculations [6]. In fact, it is not really a threshold of silica attack, yet an apparent threshold due to the difference of composition of the reaction products according to the calcium concentration as shown in [13]. The alkali concentration threshold, for which gel is no longer sufficiently expansive, is not constant as supposed in [11] but depends on the calcium concentration and the temperature, which can be approximated through the simplified approach proposed in the next part.

Equation 2 evaluates the alkali bound in ASR-gels. The molar ratio between silica (SiO2) and alkali (Na2O) present in gels in laboratory conditions is about 5. The number of ASR-gel moles produced by the reaction is assumed to be equal to the number of moles of silica attacked by alkalis.

Alkali threshold

Kim and Olek showed that the formation of ASR-gels stopped when the alkali concentration became lower than a threshold value [13]. The rate of alkali binding (Equation 2) can be read as a simplified representation using only the alkali concentration to represent the disequilibrium.

For high alkali concentration, the silica attack is rapid and large quantities of alkali are bound by gels. ASR-gel contains mainly alkali and silica [13] and is very expansive [14], [15]. For lower alkali concentration, portlandite is dissolved and calcium concentration increases. The rate of alkali binding decreases and gel becomes rich in calcium [13]. Such gels with high calcium content have low bound water contents [16] and could cause less expansion [14], [15].

In consequence, $[Na^+]^{thr}_{(Ca,T)}$, the alkali limit under which expansion stops, is not constant and has to be quantified according to the calcium concentration and the temperature. Based on the thermodynamic equilibrium of portlandite [10], calcium concentration (in mol/l) in the pore solution can be approximated from alkali concentration (in mol/l) and absolute temperature by [17]:

$$[Ca^{2+}] = 0.357 \cdot \exp(386.8 \cdot [Na^+] - 0.01 \cdot T - 1.4 \cdot [Na^+] \cdot T) \quad (3)$$

Thus, calcium concentration can be evaluated from alkali and temperature. It is not necessary to model calcium diffusion, which limits the number of different variables in the numerical resolution. Kim et al. [12] measured the evolution of alkali concentration in mortars subjected to ASR. From this experiment, it was possible to evaluate the alkali threshold at about 0.325 mol/l at 23°C. For such an alkali concentration and temperature, Equation (3) gives a calcium concentration of about 0.11 mmol/l. At 23°C, if the alkali concentration becomes lower than 0.325 mol/l, Kim et al. show that expansion stops [12]. For this limit, the $[Na^+]$ / $[Ca^{2+}]$ ratio is around 3,000. At 23°C, if the $[Na^+]$ / $[Ca^{2+}]$ ratio is higher than this ratio, alkali ions are predominant and gels are very expansive. If calcium becomes preponderant compared to alkali (ratio lower than 3,000), gels are less expansive [13]. Therefore, $[Na^+]^{thr}_{(Ca,T)}$ can be defined as:

$$[Na^+]^{thr}_{(Ca,T)} = \rho^{(T)}_{sol} \cdot [Ca^{2+}] \quad (4)$$

$\rho^{(T)}_{sol}$, the $[Na^+]$ / $[Ca^{2+}]$ limit ratio for a temperature T. This ratio depends on the different solubility constants of the species acting in these processes (silica gels with more or less alkali and calcium) and thus on temperature since the variations of the constants with temperature are different [13].

Using Kim et al.'s experimental results [12], the ratio $\rho^{(T)}_{sol}$ can be evaluated for three temperatures (23, 38 and 55°C – FIGURE 2). It is interesting to note the good agreement of the variation of $\rho^{(T)}_{sol}$ determined from Kim et al.'s experiments with the Van't Hoff law for a standard enthalpy change of 205.9 kJ/mol (FIGURE 2), with $\rho^{(293)}_{sol}$ equal to 1.54e3. This law was used to perform the following case study.

Finally, the different reactive processes involved in ASR are condensed into a single characteristic time to be calibrated on an expansion test.

Combination of transport and fixation in aggregates

Two processes are assumed to drive the kinetics of alkali-silica reaction:

- Transport in aggregate, represented by the diffusion coefficient in aggregate and;
- Reaction mechanisms (silica attack and gel formation), represented by the characteristic time of ASR for the reactions.

Kinetics is also dependent on aggregate size due to diffusion: the larger the aggregate, the slower the penetration of ions into it (whatever the diffusion coefficient). The difference of kinetics of ASR-gel formation with aggregate size is smaller for a coefficient of diffusion of 1.e-13 m²/s than for a coefficient of 1.e-14 m²/s (FIGURE 3). The difference becomes all the greater as the aggregate size grows (FIGURE 3). However, it is not possible to obtain realistic calculations for concrete containing mixes of reactive aggregate with different sizes from this transport equation alone, as shown in [10]. With the assumption that transport in aggregate totally drives ASR kinetics, calculations lead to an overestimate of the impact of the smallest reactive particles in alkali binding. Expansion of concrete containing both small and large aggregate is then underestimated [10]. If the two phenomena are taken into account and whether the transport is fast compared to the chemical reaction, ASR-gel development is proportional to bound alkali which appear to be homogeneous in the aggregate (FIGURE 4-a). Expansion is little impacted by aggregate size which is the case for aggregate with low reactivity [18]. But for more slowly diffusing aggregate with very reactive silica, gradient of bound

alkali in the aggregate can exist (FIGURE 4-b). Larger differences of expansion with aggregate size are observed [19]. In reality, the front does not necessarily start from the external limit of the aggregate as in the simplified representation used in the model. It can also be a front starting from cracks existing in the aggregates before the ASR starts as observed in [7], [20]. Pore solution and alkali can move rapidly in such cracks, while the real diffusion impacting ASR-kinetics is a slower diffusion that takes place in the natural and less connected porosity of the aggregate.

2.2 Concrete scale

Impact of alkali leaching on ASR-expansion tests have to be taken into account even in laboratory controlled conditions at 95 % relative humidity. Therefore, ASR-expansion is not a uniform phenomenon even at the scale of the specimen (FIGURE 5). The diffusion of alkali in concrete was determined by the usual mass balance:

$$p_c S_r \frac{\partial [Na^+]_c}{\partial t} = -\mathrm{div}\left(\overrightarrow{\varphi^c_{Na}}\right) + S^c_{\sum Na_b} \quad (5)$$

with p_c the concrete porosity, Sr the degree of saturation (assumed constant), $[Na+]_c$ the alkali concentration in the concrete solution, $\overrightarrow{\varphi^c_{Na}}$ the alkali flow at the specimen scale, and $S^c_{\sum Na_b}$ the sink term to account for alkali bound in ASR-gels at each time step determined at the aggregate scale. The alkali flow in concrete depends on its coefficient of diffusion in the concrete. The sink term of bound alkali can be calculated from the alkali flow in aggregate (FIGURE 1):

The equations of transport in the aggregate and of ASR reaction (Equations (1) and (2), aggregate scale) and Equation (5) of global diffusion (concrete scale) are coupled. The chemical approach proposed considers the diffusion in the specimen (top of Figure 5), takes the consumption of alkali ingress in aggregates into account (middle of Figure 5) and leads to the determination of the resulting gradient of volume of ASR-gels in the specimen (bottom of Figure 5). Due to the alkali gradient, the equations at the aggregate scale have to be solved at different points of the specimen.

3 CASE STUDY

From the volume of gels produced by the reaction, the mechanical effects on aggregate and concrete can be evaluated through the two main mechanical assumptions: imposed chemical strain or pressure. In this paper, the expansion is obtained through an existing poromechanical model previously developed and taking account of the damage and creep of concrete resulting from both external loading and internal pressure [21].

The well-documented experiment on the impact of leaching on ASR-expansion performed by Lindgård [3], [22] is now analyzed using the previous equations. In this study, the alkali leaching and expansion were both measured on the same specimens. The impact of leaching on ASR-expansion was analysed from experimental results obtained at 38°C on specimens with cross sections of 70x70 mm and 100x100 mm kept at 95% RH and soaked in water [3], [22]. Alkali leaching (FIGURE 6-a) and expansion (FIGURE 6-b) over two years were measured for the two sizes of specimens and for two moisture conditions (95% with limited leaching and in water with high leaching).

External conditions of leaching were difficult to represent. Indeed, the storage at 95% RH does not give a boundary condition that is easy to model for alkali external diffusion since such storage should not cause any leaching. In reality, leaching is due to the condensation of water vapour on the surfaces of specimens following small temperature variations during the tests. The boundary condition was obtained by inverse analysis of the total leached alkali given by experiments (FIGURE 6-a). As alkali bound by ASR-gels acts on this total amount of leached alkali, the inverse analysis of boundary conditions and the calibration of expansion parameters were performed simultaneously for the most limited leaching (specimens with cross section of 100x100 mm kept at 95% RH). Once expansion parameters had been determined for these conditions (FIGURE 6-b), only the boundary conditions were modified to obtain the other leaching curves (FIGURE 6-a) storage in water and specimens with cross sections of 70x70 mm) with no modification of the expansion parameters. With good reproduction of leaching results (FIGURE 6-a), ASR-expansions calculated by the previous equations were in good agreement with expansions measured during experiments (FIGURE 6-b). The differences of expansion for the two sizes of specimens studied in [3], [22] could be quantified by the differences of ASR-advancement in specimens (FIGURE 7). In the specimens with severe conditions of leaching, expansion stopped when the alkali concentration dropped below the alkali threshold obtained through Equations (3) and (4) about 260 mmol/l at 38°C). This analysis validated the simplified representation of the alkali threshold for the assessment of ASR-expansion in various alkali conditions. Moreover, the expansion decrease with the specimen size could then be explained by the alkali leaching itself. In

this case, it was not useful to assess the volume of gels lost by permeation through cracks as for experiments on specimens kept in NaOH solution [6]. This effect of gel permeation appeared to be negligible compared with the alkali leaching effect for the sizes of specimens and the conditions of this experiment. Lastly, modelling can assess a theoretical value of expansion which could appear in concrete if no leaching occurred (FIGURE 6-b) within the outlines of the assumptions proposed here. This value could be more representative of potential expansion for structural analysis since, in the core of large damaged structures, leaching should be negligible. However, it cannot be stated that it will represent the real expansion in damaged structures, because of environmental conditions (moisture conditions, temperature effects on viscosity and/or molar volume of ASR-gels, mechanical conditions) or other disturbing effects (gel permeation through cracks).

4 CONCLUSION

ASR expansion test results can be impacted by several different mechanisms in laboratory conditions. One of the main consequences is the difficulty of using these expansion tests results for analyzing the behaviour of ASR-damaged structures. At the aggregate scale, a mass balance equation with a sink term is necessary to obtain simplified but realistic kinetics of ASR-expansion. The alkali transport in aggregate is necessary to reproduce the dependence of the ASR kinetics on size for aggregates with high and intermediate reactivity. The sink term of binding depending on alkali concentration is necessary to represent alkali fixation and to reproduce ASR kinetics of aggregates with low reactivity and mixes of reactive aggregate of different sizes (particularly the impact of the finest reactive particles for aggregates with intermediate reactivity). The modeling used the combination of the mass balance at aggregate scale with the alkali transport at the concrete scale. It assesses the apparent alkali threshold according to temperature and calcium concentration with simplified equations. Differences of expansions on specimens in leaching conditions drawn from literature have been reproduced using the proposed equations. Due to the high mobility of alkali ions, alkali leaching should not be neglected in ASR-modelling, particularly for the analysis of expansions in specimens, since it induces a significant expansion gradient between the core and the external surface.

5 ACKNOWLEDGEMENT

The authors would like to thank Jan Lindgård for verifying the data used in part 3. 'Case Study'.

6 REFERENCES

[1] C. A. Rogers et R. D. Hooton, « Reduction in mortar and concrete expansion with reactive aggregates due to alkali leaching », *Cem Concr Agg*, vol. 13, nº 1, p. 42-49, 1991.

[2] P. Rivard, M. A. Bérubé, J. P. Ollivier, et G. Ballivy, « Alkali mass balance during the accelerated concrete prism test for alkali-aggregate reactivity », *Cem. Concr. Res.*, vol. 33, p. 1147-1153, 2003.

[3] J. Lindgård, E. J. Sellevold, M. D. A. Thomas, B. Pedersen, H. Justnes, et T. F. Rønning, « Alkali-silica reaction (ASR) - Performance testing: Influence of specimen pre-treatment, exposure conditions and prism size on alkali leaching and prism expansion », *Cem. Concr. Res.*, vol. 53, p. 68-90, 2013.

[4] S. Poyet, A. Sellier, B. Capra, G. Thèvenin-Foray, J. M. Torrenti, H. Tournier-Cognon, et E. Bourdarot, « Influence of Water on Alkali-Silica Reaction: Experimental Study and Numerical Simulations », *J. Mater. Civ. Eng.*, vol. 18, nº August, p. 588-596, 2006.

[5] D. W. Hobbs et W. H. Gutteridge, « Particle size of aggregate and its influence upon the expansion caused by the alkali–silica reaction », *Mag. Concr. Res.*, vol. 31, nº 109, p. 235-242, 1979.

[6] X. X. Gao, S. Multon, M. Cyr, et A. Sellier, « Alkali-silica reaction (ASR) expansion: Pessimum effect versus scale effect », *Cem. Concr. Res.*, vol. 44, p. 25-33, 2013.

[7] J. M. Ponce et O. R. Batic, « Different manifestations of the alkali-silica reaction in concrete according to the reaction kinetics of the reactive aggregate », *Cem. Concr. Res.*, vol. 36, p. 1148-1156, 2006.

[8] M. Ben Haha, E. Gallucci, A. Guidoum, et K. L. Scrivener, « Relation of expansion due to alkali silica reaction to the degree of reaction measured by SEM image analysis », *Cem. Concr. Res.*, vol. 37, p. 1206-1214, 2007.

[9] Y. Furusawa, H. Ohga, et T. Uomoto, « An analytical study concerning prediction of concrete expansion due to alkali–silica reaction », in *in: Malhotra (Ed.), 3rd Int. Conf. on Durability of Concrete, Nice, France*, 1994, p. 757–780, SP 145–40.

[10] S. Poyet, A. Sellier, B. Capra, G. Foray, J.-M. Torrenti, H. Cognon, et E. Bourdarot, « Chemical modelling of Alkali Silica reaction: Influence of the reactive aggregate size distribution », *Mater. Struct.*, vol. 40, p. 229-239, 2007.

[11] S. Multon, A. Sellier, et M. Cyr, « Chemo-mechanical modeling for prediction of alkali silica reaction (ASR) expansion », *Cem. Concr. Res.*, vol. 39, p. 490-500, 2009.

[12] T. Kim, J. Olek, et H. Jeong, « Alkali–silica reaction: Kinetics of chemistry of pore solution and calcium hydroxide content in cementitious system », *Cem. Concr. Res.*, vol. 71, p. 36-45, 2015.

[13] T. Kim et J. Olek, « Chemical sequence and kinetics of alkali-silica reaction part II. A thermodynamic model », *J. Am. Ceram. Soc.*, vol. 97, p. 2204-2212, 2014.

[14] T. C. Powers et H. H. Steinour, « An interpretation of some published researches on the Alkali-Aggregate Reaction - Part 1: The chemical reactions and mechanism of expansion », *J. Am. Concr. Inst.*, vol. 26, nº 6, p. 497-516, 1955.

[15] M. Prezzi, P. J. M. Monteiro, et G. Sposito, « The alkali-silica reaction, part I: Use of the double-layer theory to explain the behavior of reaction-product gels », *ACI Mater. J.*, vol. 94, nº 94, p. 10-17, 1997.

[16] A. Leemann, G. Le Saout, F. Winnefeld, D. Rentsch, et B. Lothenbach, « Alkali-Silica reaction: The Influence of calcium on silica dissolution and the formation of reaction products », *J. Am. Ceram. Soc.*, vol. 94, p. 1243-1249, 2011.

[17] M. Salgues, A. Sellier, S. Multon, E. Bourdarot, et E. Grimal, « DEF modelling based on thermodynamic equilibria and ionic transfers for structural analysis », *Eur. J. Environ. Civ. Eng.*, vol. 18, nº 4, p. 377-402, 2014.

[18] C. F. Dunant et K. L. Scrivener, « Effects of aggregate size on alkali-silica-reaction induced expansion », *Cem. Concr. Res.*, vol. 42, p. 745-751, 2012.

[19] L. F. M. Sanchez, S. Multon, A. Sellier, M. Cyr, B. Fournier, et M. Jolin, « Comparative study of a chemo–mechanical modeling for alkali silica reaction (ASR) with experimental evidences », *Constr. Build. Mater.*, vol. 72, p. 301-315, 2014.

[20] L. F. M. Sanchez, B. Fournier, M. Jolin, et J. Duchesne, « Reliable quantification of AAR damage through assessment of the Damage Rating Index (DRI) », *Cem. Concr. Res.*, vol. 67, p. 74-92, 2015.

[21] E. Grimal, A. Sellier, Y. Le Pape, et E. Bourdarot, « Creep , Shrinkage , and Anisotropic Damage in Alkali- Aggregate Reaction Swelling Mechanism — Part II : Identification of Model Parameters and Application », *ACI Mater. J.*, vol. 105, nº 105, p. 236-242, 2008.

[22] J. Lindgård, E. J. Sellevold, M. D. A. Thomas, B. Pedersen, H. Justnes, et T. F. Rønning, « Alkali-silica reaction (ASR) - Performance testing: Influence of specimen pre-treatment, exposure conditions and prism size on concrete porosity, moisture state and transport properties », *Cem. Concr. Res.*, vol. 53, p. 145-167, 2013.

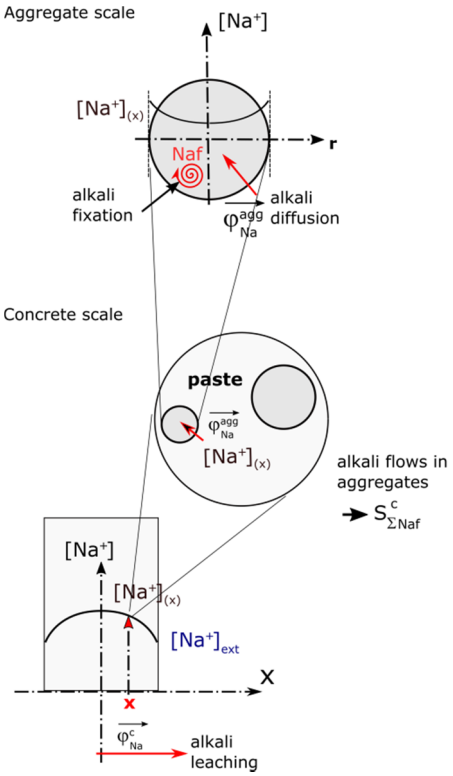

FIGURE 1: Alkali mass balance at aggregate and at concrete scale.

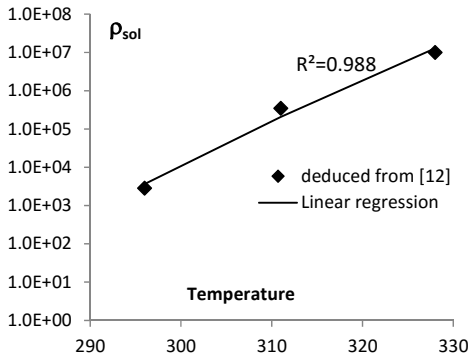

FIGURE 2: Determination of alkali threshold with temperature.

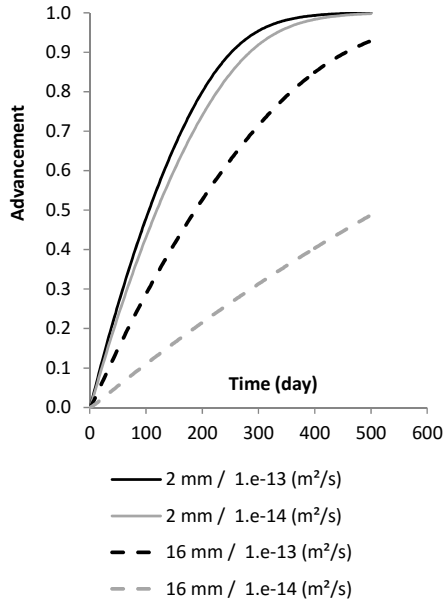

FIGURE 3: Kinetics of gel formation for two coefficients of diffusion and the same characteristic time of reaction for two sizes of aggregate (mean diameters 2 and 16 mm).

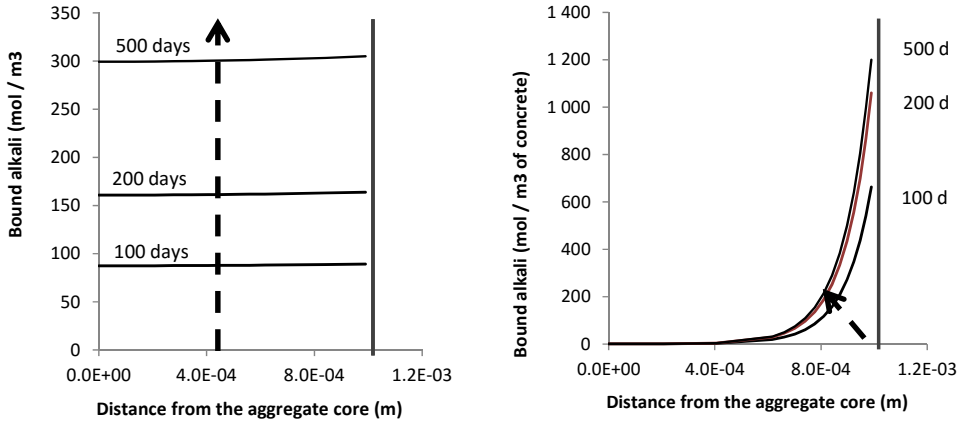

(a) (b)

FIGURE 4: Alkali bound in ASR-gels for an aggregate of mean diameter of 2 mm: (a) aggregate with slow reactivity, (b) aggregate with high reactivity.

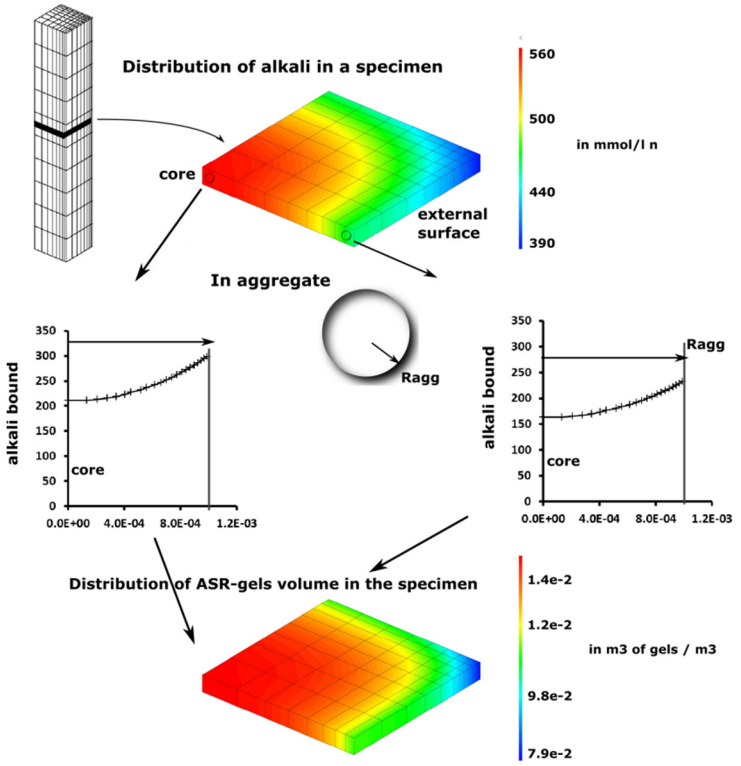

FIGURE 5: 100x100 mm cross section subjected to ASR in leaching condition. Top: distribution of alkali in specimen, middle: gradient of bound alkali in aggregates in the core and at the external surface of the specimen, bottom: resulting distribution of ASR-gels in specimen.

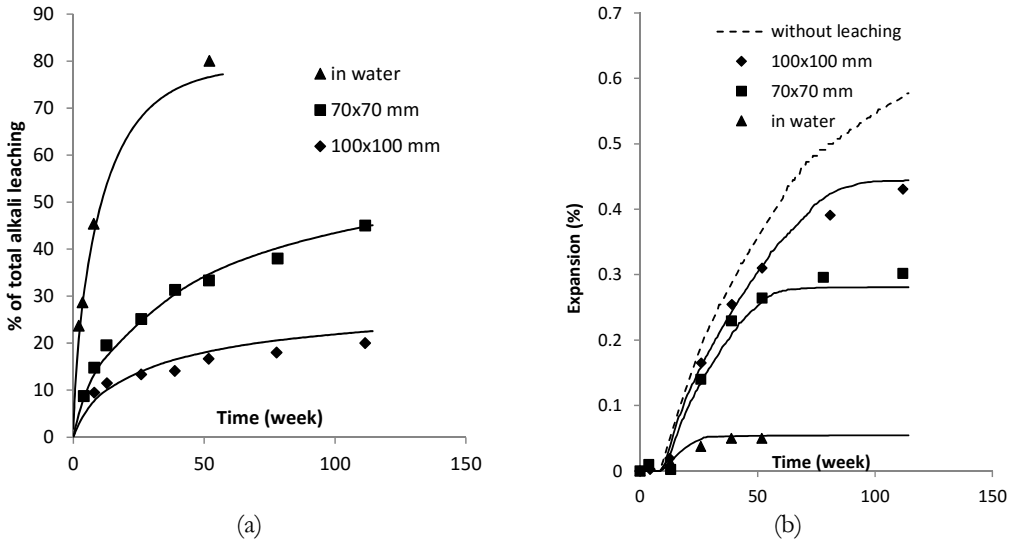

(a) (b)

FIGURE 6: Alkali leaching (a) and expansion (b) in Lindgard's experiments [3] (points) and numerical modelling (curves).

100x100 mm	70x70 mm

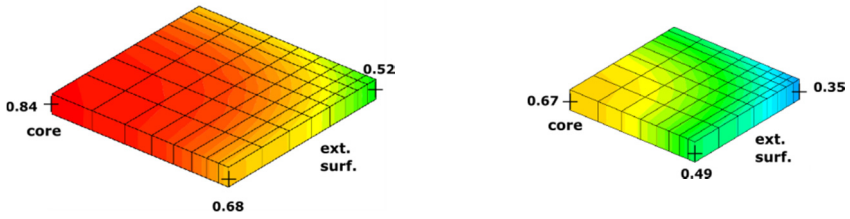

FIGURE 7: Advancement of ASR in one size of aggregate in the specimens of Lindgard's experiments [3] after 100 weeks.